ACS OMEGA

http://pubs.acs.org/journal/acsodf

Article

Simultaneous Spatiotemporal Measurement of Structural Evolution in Dynamic Complex Media

Ruitao Wu and Aristide Dogariu*

Cite This: *ACS Omega* 2022, 7, 18922−18929

Read Online

ACCESS | Metrics & More | Article Recommendations

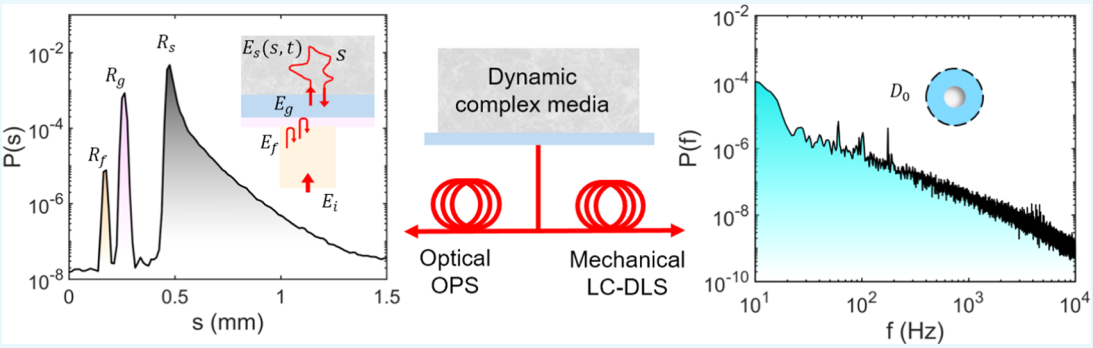

ABSTRACT: When the properties of soft materials evolve in time, the simultaneous measurement of different characteristics is critical. Here, we demonstrate an experimental system that permits monitoring both the spatial and temporal evolution of the optical and mechanical properties. An integrated fiber-optic-based system allows determining the mechanical vibrations of structural elements over 5 orders of magnitude and over a broad frequency range. At the same time, the optical properties can be obtained within seconds from high-resolution measurements of the path-length distribution of reflected light. With proper cyclical scanning, the temporal evolution of the mesoscopic light scattering properties can be obtained in a depth-resolved manner. The performance of this integrated measurement is validated in the particular case of drying paint films. For these typical nonstationary media, we show how our approach provides unique access to the spatiotemporal material properties and how this information permits identifying the specific stages of structural evolution.

INTRODUCTION

The mesoscopic structure of composite materials, including gels, paints, foams, colloids, etc., determines both their mechanical and optical properties.[1] In most cases, the structure of these materials changes in time and also varies in response to external influences such as temperature, shear stress, etc.[2] During such evolution, materials may even experience phase transitions. Understanding and controlling these spatiotemporal, multiscale processes is a tremendous task, which is mainly hindered by the difficulty to follow simultaneously the evolution of different physical properties. High-resolution characterization techniques for the mechanical and optical properties usually require separate settings and, moreover, operate at different structural scales.

The mechanical properties of soft materials are examined using a variety of rheological techniques. Conventional rheometers are usually used for measuring the low-frequency (lower than 100 Hz) viscoelastic response of bulk media.[3] To investigate the high-frequency (typically up to 100 kHz) viscoelastic moduli of materials at the microscale, active-microrheology approaches using the shear forces applied by embedded probes have been proposed and demonstrated, such as optical tweezers[4] or atomic force microscopy (AFM).[5] In certain circumstances, one can also use passive-microrheology methods, such as diffusive wave spectroscopy (DWS), which rely on tracking the movement of thermally activated particles.[6,7]

The optical properties of complex materials are usually probed at macroscales using different specular or diffusive reflectometry techniques. A well-known example is the polarized light interferometry for measuring the specular reflectance of a rough surface at a given incident angle.[8] The total diffusive reflectance of complex materials can also be evaluated using integrating sphere systems, which, when the opacity permits, can also be utilized in transmission.[9] These

Received: March 29, 2022
Accepted: May 11, 2022
Published: May 24, 2022

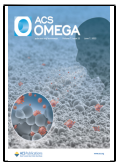

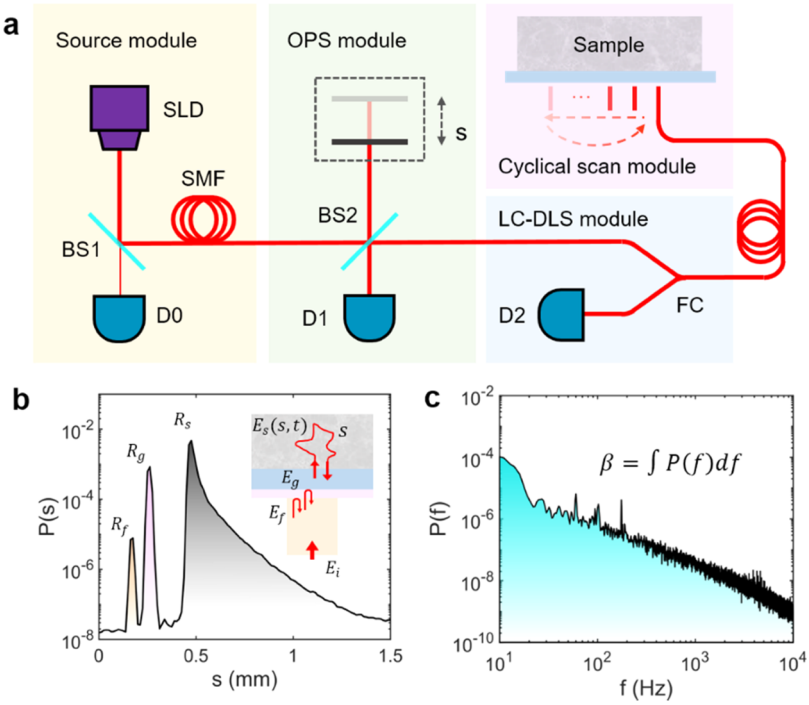

Figure 1. (a) Measurement principle and experimental setup comprising (1) superluminescent light source with intensity calibration, (2) OPS module on a Michelson interferometer with a controllable path delay, (3) LC-DLS module with a high-speed photoreceiver, and (4) a mechanical scanning module in the proximity of the medium under test. (b) Typical optical path-length distribution (OPS signal) from a highly scattering medium. (c) Typical power spectrum of intensity fluctuations (LC-DLS PSD signal) corresponding to a dynamic scattering medium.

methods reflect the structural properties averaged over scales much larger than individual scattering elements, and their interpretation requires statistical models for light−matter interaction. For instance, the effective local structure factor and scattering cross section of individual scatters can be probed by measuring the total transmittance of a slab in a diffusive regime of interaction.[10] The accuracy of such measurement will, therefore, require ergodicity and stationarity during the measurement, as well as a proper ensemble average.

To bridge this gap between separate measurements of the mechanical and optical properties, we introduce an experimental procedure that permits assessing simultaneously the spatial and temporal evolution of both optical and mechanical properties of highly dense colloidal systems. Relying on fiber-optic sensing, this technique is noninvasive to the material structure and allows us to continuously follow the nonstationary structure of complex systems. We will demonstrate the capability to follow the structural evolution with high resolution and over a broad time interval while providing a depth-resolved description of optical properties. In the following, we will examine the complex process of drying and structural phase transitions in dense colloidal systems, but the approach is applicable to the study of other nonstationary phenomena in composite media.

METHODS

Measurement Principle and Setup. The measurement apparatus consists of four different independent modules, as schematically depicted in Figure 1a. The modules, which include the source, optical path-length spectroscopy (OPS), low-coherence dynamic light scattering (LC-DLS), and the cyclical scan, are physically interconnected through single-mode fibers (SMFs).

The source module consists of a fiber-coupled superluminescent diode (SLD) with a coherence length of 30 μm (Superlum, cBLMD-S-670-HP1-SM-1). The light from the SLD is subsequently split into two using a 99/1 splitter (BS1), while a minimum amount of the power is directed to a power detector D0 (New Focus, 2153 Photo Receiver) for intensity calibration. Most of the light power is sent to the other modules for measurement.

The second module is the OPS module, which provides a high-resolution time-resolved reflection signal analysis from the sample. The OPS module is a fiber-based Michelson interferometer, as introduced in our previous works.[11] Briefly, light from the source module is split into two paths using a 50/50 splitter (BS2). The scanning mirror on the reference arm is controlled to adjust the path-length delay (s) between two signals. The sample arm, as discussed later, receives the reflection from the sample and will generate an interferogram with the reference signal when the path-length delay is smaller than the coherence length of the source (30 μm). After scanning over different path lengths, using the magnitude of the interferogram at the detector (D1) side, one can calculate the flux of photons traveling within the sample of various delays. The OPS measurement provides the probability distribution of optical path lengths, namely, the $P(s)$, within the medium. A typical example of $P(s)$ is shown in Figure 1b, while the inset shows the reflection from different optical path lengths, which includes Fresnel reflection from the fiber facet and the glass interface, as well as the scattered light within the sample. As we will discuss in the next section, the $P(s)$ analysis provides ample information about the optical properties of the medium.

The third LC-DLS module consists of a fiber coupler (FC) and a high-speed photon receiver (D2, New Focus, 2011-FC).

https://doi.org/10.1021/acsomega.2c01915
ACS Omega 2022, 7, 18922−18929

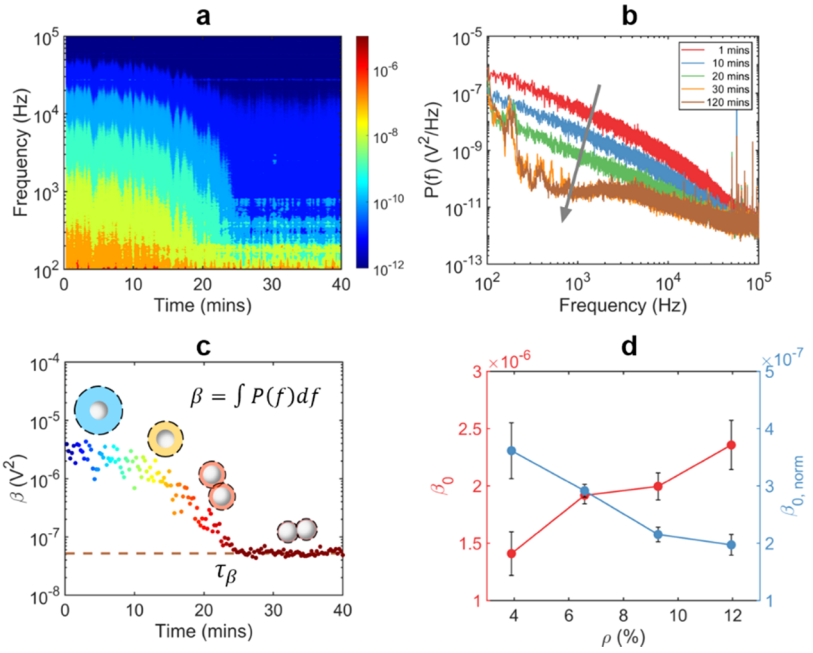

Figure 2. Mechanical information obtained from LC-DLS measurements. (a) The time-evolving PSDs contour during the drying process of a paint film. (b) Representative PSDs in panel (a). The arrow indicates the increase in the measurement time. (c) The time-evolving scatter dynamics in a nonstationary medium. The inset denotes the diffusivity of the scatters. (d) The strength of the initial dynamics for media with different scatter concentrations. Left: total dynamics β_0. Right: normalized dynamics w.r.t. scatter concentration $\beta_{0,\mathrm{norm}}$. Error bars represent the data from four identically prepared samples.

The LC-DLS module has two main advantages. First, it uses the heterodyne detection technique by interferencing of the local reflected signal with the scattered light to amplify the signal. Second, the use of low coherence light will minimize the effect of multiple scattering and effectively capture only the contribution of the sample signal within the coherence length in front of the probe. A detailed discussion on the LC-DLS technique can be found elsewhere.[12] For this particular measurement, the LC-DLS module gives $P(f)$, which is the power spectrum density (PSD) of the reflected fluctuating light. The integration of the PSD over the frequency domain, which is represented by β, gives the total energy of the fluctuating signal.

Finally, a controlled scanning across the sample under test is realized using a movable SMF optical fiber probe for simultaneously illuminating the sample and capturing the reflected light. The SMFs sets on a motorized stage (Newport 460A-XY) under the control of a three-axis motion controller (Newport, EPS300), allowing for a high-spatial-resolution scanning across the sample surface. The information of the sample, which is encoded in the reflected scattered light, is sent to both the OPS and the LC-DLS modules for further analysis. The fact that the measurements rely on one endoscopic-like fiber probe of 125 μm in diameter for detection provides the feasibility and convenience for in situ measurements.

We note that all of the motion control, data acquisition, and analysis are performed simultaneously and automatically operated using MATLAB and LabVIEW environments. All being fiber-optic-based, this compact system is flexible, robust, and mechanically stable.

Sample Preparation. As generic examples of nonstationary scattering media, in this paper, we use a series of drying paint films on glass substrates. The samples are commercially available as water-based white paint films with different physical properties. Two series of samples are examined and discussed. The first series includes four different concentrations of titanium dioxide, with a volume fraction ranging from 3.9 to 11.95%. As for the second series, which consists of also four samples, they shared the same level of scatters (10%), with varying coalescent properties. This is achieved by adding different levels of coalescent agents (volume percentage from 0 to 2%) into the paint. The other properties are maintained the same by adding water correspondingly to maintain the same dilution ratio.

Measurement Procedure. Each sample consists of a paint film with a 170 μm thickness applied on a coverslip using a drawdown bar of 1 inch width. Index-matching oil was used between the optical fiber and the bottom of the coverslip. The sample was then placed on the sample stage (final module). The distance between the probing fiber and the bottom of the glass was 100 μm. For each measurement, we performed a cyclical spatial scanning procedure. For each cycle, we implemented a one-dimensional spatial scanning of the fiber probe with a 20 μm step size over 100 positions. The probe stays at each position for around 6 s, allowing sufficient time for the OPS module to scan over a 4 mm optical path-length range (with a 300 fs temporal resolution). Right after finishing each cycle, the probe is retracted to the initial position for the next cycle. The total duration of each measurement is 2 h, which consists of 12 spatial scanning cycles. The goal of this cyclical scanning process is to obtain a depth-resolved reflection signal over different positions and investigate its temporal evolution properties. On the other side, the LC-DLS module continuously measures the fluctuating signal over the mechanical vibration frequency from the scatters within the sample, with a 15 s integration time. The frequency of the PSD ranges from 1 to 10 kHz, with a 1 Hz resolution, which provides high-resolution mechanical information of the

https://doi.org/10.1021/acsomega.2c01915
ACS Omega 2022, 7, 18922−18929

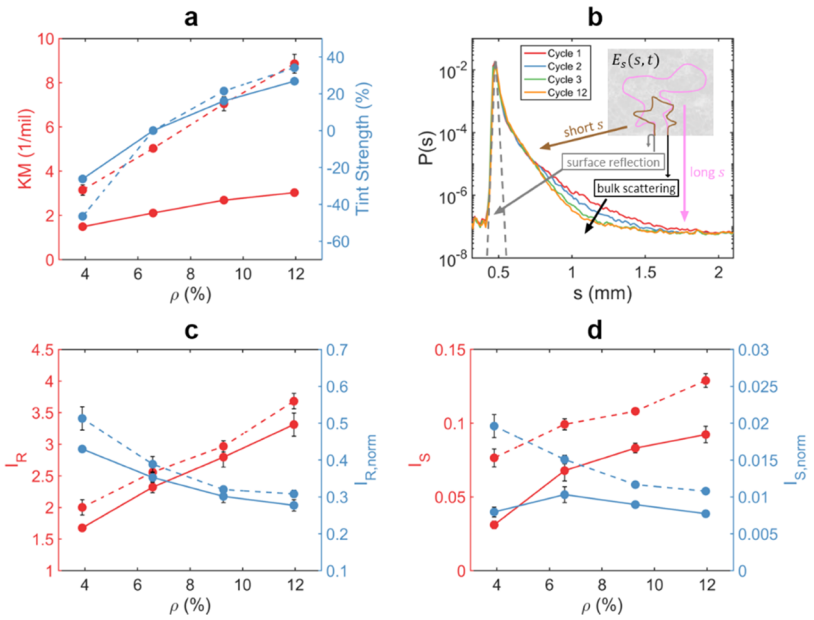

Figure 3. Optical information retrieved from OPS measurements. (a) Characteristic of all samples with the standard light scattering technique. Left: KM (Kubelka–Munk). Right: TS (tint strength). (b) Representative $P(s)$ for a nonstationary complex medium. The OPS approach can distinguish the surface reflection (gray arrow) and bulk scattering (black arrow) with different path lengths s. The surface reflection I_R (c) and bulk scattering I_s (d) of different complex media at the wet stage (dotted lines) and dried stage (solid lines) before (left) and after (right) normalizing with the scatters' concentration. Error bars represent the data from four identically prepared samples.

dynamic scattering sample. Each sample is repeated four times to obtain sufficient statistical averaging.

We note that all of the measurement parameters, including spatial resolution, sampling rate, spatial number, cycle number, etc., can be easily adjusted according to the specific physical properties of the sample. Also, the modular design of the current system also permits integration with other measurement techniques, such as reflectometry,[8] complementing LSI with infrared spectroscopy,[13] etc.

RESULTS AND DISCUSSION

Mechanical Properties of Drying Media. As mentioned before, the LC-DLS measurement provides information regarding the mechanical dynamics of the scattering centers within the medium.[12] We demonstrate this using a typical nonstationary dynamic medium, i.e., a drying paint film, in which the phases of the drying process evolve in time. When the medium is illuminated, the mechanical dynamics of the titanium dioxide particles are encoded into the intensity fluctuation of the reflected speckle patterns. With our experimental design, the detector captures the interference of the reflected light from the glass–medium interface and the scattered light within the coherence volume (~100 fL) at the end of the fiber probe. By analyzing the intensity–intensity correlation function in the frequency domain, one can further infer the dynamical information of the particles. There are two parameters associated with the PSD, the overall magnitude of $P(f)$ and the characteristic frequency. The overall magnitude represents the total energy from the dynamic light, which is evaluated as $\beta = \int P(f)\mathrm{d}f$. This parameter is proportional to the total number of scatters and the diffusivity of a single scatter.[14] The characteristic frequency, on the other hand, is directly associated with the diffusivity of each particle, which is affected by the particle size, the particle shape, the viscoelasticity of its environment, etc.[15] For the example of the drying paint film, the scatters initially manifest a Brownian-type motion in a viscoelastic medium but then they gradually lose their mobility and finally freeze. We demonstrate the capability of this system to detect the mechanical information from samples of different scattering strengths (first series of the sample). The results are summarized in Figure 2.

Figure 2a shows the contour of PSDs over the first 40 min of the measurement. A few selected PSDs are also plotted in Figure 2b to illustrate their time evolution properties. The magnitudes of the PSDs decrease over the measurement time, which is a clear indication of the drying process. When the paint film freezes completely around 25 min, the measured PSDs will remain the same in magnitude and shape, which is the background of the measurements (mainly contains mechanical vibration of the system and electronic noise of the detectors).

As mentioned earlier, a critical descriptor for the diffusivity/mobility of the scatters is the strength of the dynamics, which is denoted by β and calculated by integrating the PSD over the mechanical frequency regime. Practically, β integrates over a smaller frequency band (6–10 kHz) to minimize the effect of mechanical vibration and electronic noise. As illustrated in Figure 2c, β has a relatively constant value initially (around 5 min), meaning each scatter within the sample has been diffusing independently. Later on, the effective diffusivity of each scatter will decrease due to the interparticle hydrodynamic interaction, which is supported by the decreasing β.[16] Finally, β reaches a constant value, as the scatters have lost their mobility completely. This characteristic time has a critical physical meaning, which is marked as τ_β and will be discussed in detail in later sections.

We note that the concentration of the scatters affects β. Therefore, it is feasible to retrieve the scatter density by comparing samples of different scatter concentrations, as demonstrated in Figure 2d. On the left axis, we showed β_0, which is the total dynamics averaged over the first 5 min. At

https://doi.org/10.1021/acsomega.2c01915
ACS Omega 2022, 7, 18922–18929

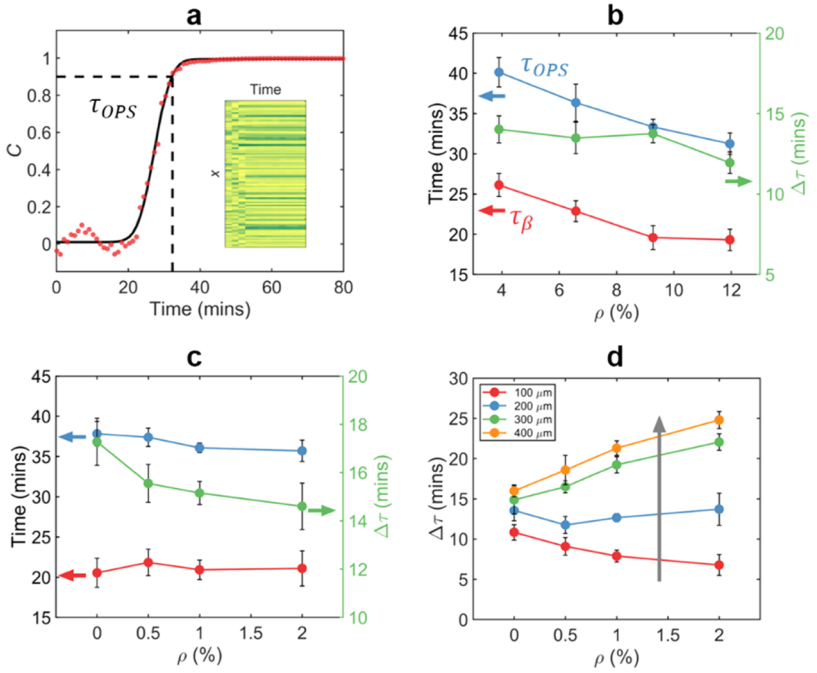

Figure 4. Drying time retrieved through the measurement. (a) τ_{OPS} calculated from the time-evolving correlation coefficient of the scattered light. Inset: example of a spatiotemporal distribution of the total reflected light from one medium. (b) Measurements of the drying times for different complex media with varying scatter concentrations. Left: the optical drying time τ_{OPS} from panel (a) (blue dots) and mechanical drying time τ_β from Figure 2c. Right: the difference between these two drying times. (c) Similar to panel (b) but measurements taken on complex media with different levels of coalescent agents. (d) $\Delta\tau$ calculated for different depths for media with different coalescent agents. The arrow indicates the increasing path lengths s. Error bars represent the data from four identically prepared samples.

this stage of the drying process, the magnitude of dynamics is given as $\beta_0 \propto \rho D_0$, where ρ is the scatter number concentration and D_0 is the diffusivity of a single scatter.[17] As β_0 would have a higher value if the samples have more scatters, it is also critical to compare the normalized total dynamics, $\beta_{0,norm} = \beta_0/\rho \propto D_0$, as shown on the right axis. It is easy to understand the decreasing trend of $\beta_{0,norm}$ since D_0 would decrease with high concentration as the hydrodynamic interaction among the scatters at this condition would decrease the diffusivity of one scatter.[16] This also suggests the possibility of monitoring over the whole process of the scatter density ρ using a calibration measurement or quantifying D_0 with additional measurement on ρ.

Depth-Resolved Optical Properties. The capability to monitor the optical properties of a nonstationary scattering medium is provided by the OPS measurement. Here, by optical properties, we mean all of the information can be retrieved from the optical path-length distribution $P(s)$. Since $P(s)$ represents the relative contributions of light that has been scattered along paths with different delay times, at least two types of descriptors can be extracted. The first one is $I = \int P(s)ds$ and represents the total scattered light. For media interacting with light in a multiple scattering regime, the light propagation is commonly described by the diffusion equation. Under diffusion approximation, when the geometry of the system is known, for instance, a slab of finite thickness, the measured $P(s)$ can be used to extract structural parameters, such as the refractive index mismatch of the medium interface, the transport mean free path, the thickness, etc.[18,19] In the current paper, we demonstrate another exclusive feature of such a measurement: the capability to distinguish between surface reflection and bulk scattering. Furthermore, in the next section, we show how the depth-resolved optical properties can also be used to characterize the drying time of the paint film. We note that for other optical properties of interest, such as the effective refractive index of different path lengths, the diffusion approximation is not necessary. In that case, the sample thickness only needs to be larger than the coherence length of the source.

First, we carried out a conventional approach for analyzing the optical properties of the paint film under both wet and dry conditions. The Kubelka–Munk (KM)[20] and tint strength (TS),[21] which are both characteristics of the scattering strength, are measured and shown in Figure 3a. Note that for the tint strength measurement, the sample with a 6.58% volume fraction is used as the control sample. Next, in Figure 3b, $P(s)$ signals from the sample (6.58% volume fraction) at different cycles are presented. As the measurement proceeds, the $P(s)$ signal is weaker in the long optical path, which is a clear indication of the total thickness decreasing during drying. On the other hand, the reflection from the short s does not significantly alter.

With measured $P(s)$, the light reflected by the surface or scattered within the bulk can both be quantified, which is beyond the aforementioned conventional hiding measurement approaches. It would be interesting to see how the surface of a paint film plays a role for samples of different scattering strengths. In Figure 3c, we calculate the surface reflection (I_R) by integrating over the peak at s = 0.5 mm (gray dashed lines in Figure 3b) within the coherence length of the source at both completely wet (first and second cycles) and dried (last two cycles) stages of the paint. The effect of each scatter is taken care of by calculating the normalized surface reflection, $I_{R,norm} = I_R/\rho$. Similarly, the bulk scattering descriptors, I_S and $I_{S,norm} = I_S/\rho$, are also calculated and presented in Figure 3d. First, the surface of the paint film is the dominant component, and it

https://doi.org/10.1021/acsomega.2c01915
ACS Omega 2022, 7, 18922−18929

correlates with the conventional approach very well. Also, with increasing ρ, both the surface reflection and bulk scattering will enhance. The fact that the normalized scattering strength of each scatter is lower in the sample with higher ρ is due to the collective scattering effect.[10]

We note that the $P(s)$ measurement at each position takes less than 6 s. Therefore, with sufficient ensemble averaging, the OPS module can also be used to continuously monitor the temporal evolution of light scattering in nonstationary scattering media in different path lengths, which cannot be accomplished with conventional approaches (KM and TS). As we will show in the next section, this also allows retrieving the depth-resolved drying time determined by the optical properties.

Characterization of Nonstationary Processes: Drying Times and Phase Transition. As mentioned in the previous sections, the LC-DLS and OPS modules independently measure the microscale mechanical and optical information of the nonstationary scattering media, respectively, through the same fiber probe. We will now show how this capability can be used for characterizing a typical nonstationary problem of structural evolution. A particularly interesting problem would be to identify the characteristic times and the phases of drying paint films.[22] Previously, several techniques and systems have been suggested for studying the problem of a drying paint film; most of them are based on the concept of multispeckle diffusive wave spectroscopy (MS-DWS),[23] which address the particular aspect of mechanical dynamics.[24,25] As such, these approaches use the "drying time" associated with different decorrelation times, which are determined only by the dynamics of scatterers at scales.[24] Although the possible relation between these decorrelation times and different drying stages has been speculated and discussed, how they actually associate with the actual physical process remains unclear.[26] Furthermore, the role of the optical property variation has not been addressed in this context. More importantly, these approaches do not have access to depth-resolved information, which significantly limits the information about the drying process. In the following, we will show that our capability of simultaneously measuring the mechanical and optical information will provide new perspectives on the drying problem.

We start by defining two different parameters to quantify the drying process corresponding to the different physical properties of the paint film. The first one is τ_β, which represents the time when the mechanical vibration of the scatters ceases. This is the typical time scale that the DWS-type measurement focuses on. The second characteristic is τ_{OPS}, which indicates the time when the reflectivity of the paint film becomes constant. Obviously, in practical scenarios, $\tau_{OPS} \geq \tau_\beta$. This is because the reflectivity changes not only due to the scatter mobility but also due to the variation of other effects such as changes in the refractive index and the final coalescence of the paint film. This time scale is expected to be very long, practically more than 10 s, reaching a regime where no time correlation of the speckles can be measured using traditional DWS-based approaches.

Figure 4a illustrates the procedure to calculate τ_{OPS}. First, the temporal evolution of the local reflected intensity of paint $I(x, t) = \int P(x, t, s)ds$ is calculated (see the inset).

Later, Pearson's coefficient over different cycles is calculated using $C(t) = I(x, t)I_{REF}(x)/\sqrt{I(x, t)I_{REF}(x)}$. Here, $I_{REF}(x)$ is the referenced dried reflected pattern and is calculated using the averaging reflected intensity over the last six cycles. To enhance the accuracy of extracting the τ_{OPS}, the experimental data is further fitted by a modified error function $C_{fit}(t) = [\mathrm{erf}(t + a) + 1]/2$, where $\mathrm{erf}(t)$ is the error function and a is the time-offset parameter. Finally, we define the characteristic time for which the fitting function $C_{fit}(t) = 0.9$, as the moment where the optical properties do not change anymore.

As for τ_β, the approach to extracting this mechanical characteristic time is already described in Figure 2c. Since τ_β is a parameter that quantifies the time when β reaches a constant, it means that all of the mechanical vibrations of the scatters have stopped. In Figure 4b, we showed the τ_{OPS} and τ_β for the paint film with different concentrations of scatters. We observed a decrease in the drying time in both τ_{OPS} and τ_β when increasing scatterer concentrations, which is consistent with the fact that the water percentage is decreasing.

It would be interesting to see if this technique is sensitive to other factors that modify the drying properties or not, such as different coalescent agents. The coalescent agents can accelerate the process of paint coalescent, which, in principle, would change the τ_{OPS}, but keep the τ_β to remain the same, as it would not significantly modify the mechanical property. Therefore, we prepared samples of different coalescent agents with the same scatter concentration, meaning they share similar optical properties at each phase, but the time scale for stages should be different. The measurement results are summarized in Figure 4c. Note that the x axis represents the concentration of the coalescent agents. It is clear that τ_β is similar among the samples, as the mechanical properties are identical, while τ_{OPS} varies for different samples, which is a clear indication that the coalescent agents have modified the time to reach the steady state (completely dried). To better visualize this, we also calculate and plot the difference over these two time scales $\Delta\tau = \tau_{OPS} - \tau_\beta$. The addition of coalescent agents has unambiguously sped up the drying process by decreasing $\Delta\tau$, without perturbing the mechanical properties.

A significant feature of our system is that both τ_{OPS} and $\Delta\tau$ can also be obtained for different depths if proper optical path length is selected for calculating the reflectivity. An example is shown in Figure 4d, where reflectivity is integrated over every 100 μm (starting from the peak s = 0.5 mm) that is calculated. It clearly indicates that the drying time defined by the optical properties depends on the medium depth. The capability of our system to resolve the optical properties at different depths would be of great potential for solving various practical problems, for instance, identifying different drying architectures for colloidal mixtures.[27]

The two time scales τ_β and τ_{OPS} reflect different aspects of the structural evolution during the drying phases, as summarized in Figure 5. The nonstationary process of drying is characterized by different stages typically known as (1) free evaporation, (2) packing, (3) deformation and short-term coalescence, and (4) long-term coalescent process.[26] During stages (1) and (2), the mechanical movement of the scatters dominates and is well captured by the LC-DLS module with very high temporal resolution (from 0.01 ms to 1 s). These two stages can further be distinguished and separated, using the slope of β, which should correspond to the time scale of substages during the drying process.[24] The end point of the β decay defines the time when the movement of the scatters has completely stopped. After that, the deformation and short-term

https://doi.org/10.1021/acsomega.2c01915
ACS Omega 2022, 7, 18922−18929

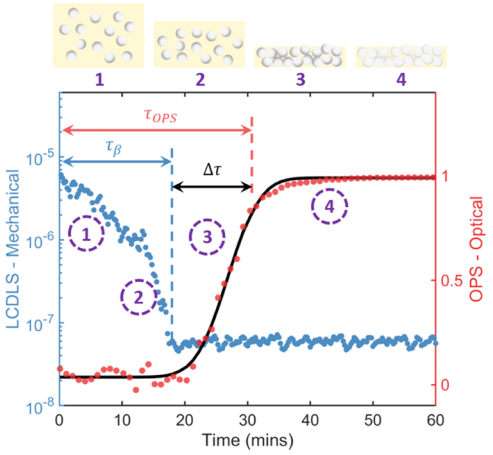

Figure 5. Measurement and its relation to the phase of the drying process. The LC-DLS technique gives the mechanical property, which is associated with the free evaporation (1) and packing (2) phases. The OPS measurements capture the time-evolving optical property and can be used to determine the deformation and the short-term coalescent process (3).

coalescent process continue to modify the optical properties of the film. The duration of this process is measured by $\Delta\tau = \tau_{OPS} - \tau_\beta$, which can only be determined by our simultaneous measurement of the optical and mechanical properties. After that, other long-term coalescent processes might still take place but without significant modification of either the optical or mechanical properties.

CONCLUSIONS

In summary, we introduced a light scattering-based system that permits characterizing simultaneously the optical and mechanical properties of scattering media. The fiber-optic probe allows recovering mechanical vibrations over frequency ranges extended more than 5 orders of magnitude. This offers the possibility to continuously monitor the dynamics of colloidal elements with a subminute temporal resolution during the extended periods of structural evolution. The optical properties of the same complex medium are determined using the same optical probe to rapidly measure the path-length distribution of the reflected intensity with a 10 μm depth resolution. A cyclical scanning module allows high-resolution and comprehensive analysis of reflected light in both spatial and temporal domains.

We illustrate the performance in the case of a typical nonstationary medium, a drying paint film with a continuously evolving microscopic structure. We demonstrated how this integrated measurement offers comprehensive information about the complex medium, including scatter density, scatter diffusivity, separation of surface reflection and bulk scattering, depth-dependent evolution of light scattering properties, etc. Moreover, the unique ability to identify specific time scales for both mechanical and optical properties of the same medium provides an inclusive description of film drying and identifies the specific stages of coalescence during the process that could not be available based on traditional measurements. Such a capability allows us to control the evolution of the physical processes and to optimize the ultimate paint properties.[22,28,29]

We would also like to compare our system with other similar approaches, especially the commonly used DWS-type system.[25] As mentioned before, the DWS-type system can also be used for measuring the mechanical properties of the paint films.[23] However, such systems do not characterize the optical properties of the medium, not to mention the depth-resolved properties. As a result, our system provides in situ information of the medium, while the signal from the DWS system is integrated over a large depth and very susceptible to the properties of the surface.[24] It should also be pointed out that our system required the fiber probe to be in certain geometries, such as that measured through a glass (as demonstrated in this paper) or inside the sample, which is not required by conventional DWS methods.

Finally, we would like to comment on the broader applicability of this type of measurement. Aside from full monitoring of drying processes, as demonstrated here, the proposed approach may find applications in a variety of situations where spatiotemporal measurements are necessary to characterize the evolution of the complex material system. For instance, it has been shown that LC-DLS measurements are effective in monitoring the spatially resolved viscoelastic moduli of the complex fluid[15] or characterizing the size evolution within a Newtonian fluid even when strong absorption presents.[12,30] On the other hand, many intricate optical properties specific to complex media such as the transport mean free path,[31] the boundary conditions,[19] or the depth-resolved intensity statistics[32] are revealed by OPS measurements. OPS measurements can also be used, in general, for monitoring the optical inhomogeneity with complex systems (dynamic or static), which can be the depth-resolved refractive index distribution in liquid mixtures[12] or inhomogeneous distribution of particles within the colloidal systems due to external forces,[33] just to name a few. Thus, the possibility to simultaneously access all of these optical and mechanical properties should be highly relevant for monitoring and characterizing soft materials such as liquid-crystalline physical gels,[34] photon/thermal-responsive materials,[35] etc., where the complex structure evolves in time or in response to various external influences. Furthermore, the ability to isolate and determine the depth-resolved properties is a unique feature, which can be critical when attempting to track the stratification dynamics of colloidal mixtures and to test the dynamical density functional theories in different practical situations.[27,36]

AUTHOR INFORMATION

Corresponding Author

Aristide Dogariu − *CREOL, The College of Optics and Photonics, University of Central Florida, Orlando, Florida 32816, United States;* orcid.org/0000-0002-2709-9632; Email: adogariu@ucf.edu

Author

Ruitao Wu − *CREOL, The College of Optics and Photonics, University of Central Florida, Orlando, Florida 32816, United States;* orcid.org/0000-0002-5801-1162

Complete contact information is available at: https://pubs.acs.org/10.1021/acsomega.2c01915

Notes

The authors declare no competing financial interest.

ACKNOWLEDGMENTS

The authors would like to thank Jose Rafael Guzman-Sepulveda for the help in building the LC-DLS module of the system.

https://doi.org/10.1021/acsomega.2c01915
ACS Omega 2022, 7, 18922−18929

REFERENCES

(1) Clyne, T. W.; Hull, D. *An Introduction to Composite Materials*; Cambridge University Press, 2019.
(2) Campbell, F. C. *Structural Composite Materials*; ASM International, 2010.
(3) Chen, D. T.; Wen, Q.; Janmey, P. A.; Crocker, J. C.; Yodh, A. G. Rheology of Soft Materials. *Annu. Rev. Condens. Matter Phys.* **2010**, *1*, 301−322.
(4) Yao, A.; Tassieri, M.; Padgett, M.; Cooper, J. Microrheology with Optical Tweezers. *Lab Chip* **2009**, *9*, 2568−2575.
(5) Alcaraz, J.; Buscemi, L.; Grabulosa, M.; Trepat, X.; Fabry, B.; Farré, R.; Navajas, D. Microrheology of Human Lung Epithelial Cells Measured by Atomic Force Microscopy. *Biophys. J.* **2003**, *84*, 2071−2079.
(6) Mason, T. G.; Weitz, D. A. Optical Measurements of Frequency-Dependent Linear Viscoelastic Moduli of Complex Fluids. *Phys. Rev. Lett.* **1995**, *74*, No. 1250.
(7) Cicuta, P.; Donald, A. M. Microrheology: A Review of the Method and Applications. *Soft Matter* **2007**, *3*, 1449−1455.
(8) Elton, N. J.; Legrix, A. Reflectometry of Drying Latex Paint. *J. Coat. Technol. Res.* **2014**, *11*, 185−197.
(9) Hanssen, L. Integrating-Sphere System and Method for Absolute Measurement of Transmittance, Reflectance, and Absorptance of Specular Samples. *Appl. Opt.* **2001**, *40*, 3196−3204.
(10) Saulnier, P. M.; Zinkin, M.; Watson, G. Scatterer Correlation Effects on Photon Transport in Dense Random Media. *Phys. Rev. B* **1990**, *42*, No. 2621.
(11) Popescu, G.; Dogariu, A. Optical Path-Length Spectroscopy of Wave Propagation in Random Media. *Opt. Lett.* **1999**, *24*, 442−444.
(12) Guzman-Sepulveda, J. R.; Dogariu, A. Probing Complex Dynamics with Spatiotemporal Coherence-Gated Dls. *Appl. Opt.* **2019**, *58*, D76−D90.
(13) Faccia, P.; Pardini, O.; Amalvy, J.; Cap, N.; Grumel, E.; Arizaga, R.; Trivi, M. Differentiation of the Drying Time of Paints by Dynamic Speckle Interferometry. *Prog. Org. Coat.* **2009**, *64*, 350−355.
(14) Popescu, G.; Dogariu, A. Dynamic Light Scattering in Localized Coherence Volumes. *Opt. Lett.* **2001**, *26*, 551−553.
(15) Sohn, I.; Rajagopalan, R.; Dogariu, A. Spatially Resolved Microrheology through a Liquid/Liquid Interface. *J. Colloid Interface Sci.* **2004**, *269*, 503−513.
(16) Batchelor, G. K. Brownian Diffusion of Particles with Hydrodynamic Interaction. *J. Fluid Mech.* **1976**, *74*, 1−29.
(17) Guzman-Sepulveda, J. R.; Wu, R.; Dogariu, A. Continuous Optical Measurement of Internal Dynamics in Drying Colloidal Droplets. *J. Phys. Chem. B* **2021**, *125*, 13533−13541.
(18) Patterson, M. S.; Chance, B.; Wilson, B. C. Time Resolved Reflectance and Transmittance for the Noninvasive Measurement of Tissue Optical Properties. *Appl. Opt.* **1989**, *28*, 2331−2336.
(19) Popescu, G.; Mujat, C.; Dogariu, A. Evidence of Scattering Anisotropy Effects on Boundary Conditions of the Diffusion Equation. *Phys. Rev. E* **2000**, *61*, 4523.
(20) Orel, Z. C.; Gunde, M. K.; Orel, B. Application of the Kubelka-Munk Theory for the Determination of the Optical Properties of Solar Absorbing Paints. *Prog. Org. Coat.* **1997**, *30*, 59−66.
(21) Gangakhedkar, N. Colour Measurement of Paint Films and Coatings. In *Colour Measurement*; Elsevier, 2010; pp 279−311.
(22) van der Kooij, H. M.; Sprakel, J. Watching Paint Dry; More Exciting Than It Seems. *Soft Matter* **2015**, *11*, 6353−6359.
(23) Lee, J. Y.; Hwang, J. W.; Jung, H. W.; Kim, S. H.; Lee, S. J.; Yoon, K.; Weitz, D. A. Fast Dynamics and Relaxation of Colloidal Drops During the Drying Process Using Multispeckle Diffusing Wave Spectroscopy. *Langmuir* **2013**, *29*, 861−866.
(24) Zakharov, P.; Scheffold, F. Monitoring Spatially Heterogeneous Dynamics in a Drying Colloidal Thin Film. *Soft Mater.* **2010**, *8*, 102−113.
(25) Van Der Kooij, H. M.; Fokkink, R.; Van Der Gucht, J.; Sprakel, J. Quantitative Imaging of Heterogeneous Dynamics in Drying and Aging Paints. *Sci. Rep.* **2016**, *6*, No. 34383.
(26) Brun, A.; Dihang, H.; Brunel, L. Film Formation of Coatings Studied by Diffusing-Wave Spectroscopy. *Prog. Org. Coat.* **2008**, *61*, 181−191.
(27) He, B.; Martin-Fabiani, I.; Roth, R.; Tóth, G. I.; Archer, A. J. Dynamical Density Functional Theory for the Drying and Stratification of Binary Colloidal Dispersions. *Langmuir* **2021**, *37*, 1399−1409.
(28) Van Der Kooij, H. M.; Van De Kerkhof, G. T.; Sprakel, J. A Mechanistic View of Drying Suspension Droplets. *Soft Matter* **2016**, *12*, 2858−2867.
(29) Lambourne, R.; Strivens, T. A. *Paint and Surface Coatings: Theory and Practice*; Elsevier, 1999.
(30) Wu, R.; Guzman-Sepulveda, J.; Kalra, A.; Tuszynski, J.; Dogariu, A. Thermal Hysteresis in Microtubule Assembly/Disassembly Dynamics: The Aging-Induced Degradation of Tubulin Dimers. *Biochem. Biophys. Rep.* **2022**, *29*, No. 101199.
(31) Douglass, K. M.; Dogariu, A. Measuring Diffusion Coefficients Independently of Boundary Conditions. *Opt. Lett.* **2009**, *34*, 3379−3381.
(32) Wu, R.; Dogariu, A. Nonstationary Intensity Statistics in Diffusive Waves. *Phys. Rev. Lett.* **2020**, *125*, No. 043902.
(33) Acevedo, C. H.; Wu, R.; Miller, J. K.; Johnson, E. G.; Dogariu, A. Colloidal Density Control with Bessel−Gauss Beams. *Sci. Rep.* **2021**, *11*, No. 12284.
(34) Bi, S.; Peng, H.; Long, S.; Ni, M.; Liao, Y.; Yang, Y.; Xue, Z.; Xie, X. High Modulus and Low-Voltage Driving Nematic Liquid-Crystalline Physical Gels for Light-Scattering Displays. *Soft Matter* **2013**, *9*, 7718−7725.
(35) Tamate, R.; Usui, R.; Hashimoto, K.; Kitazawa, Y.; Kokubo, H.; Watanabe, M. Photo/Thermoresponsive Abc Triblock Copolymer-Based Ion Gels: Photoinduced Structural Transitions. *Soft Matter* **2018**, *14*, 9088−9095.
(36) Fortini, A.; Martín-Fabiani, I.; De La Haye, J. L.; Dugas, P.-Y.; Lansalot, M.; D'agosto, F.; Bourgeat-Lami, E.; Keddie, J. L.; Sear, R. P. Dynamic Stratification in Drying Films of Colloidal Mixtures. *Phys. Rev. Lett.* **2016**, *116*, No. 118301.

https://doi.org/10.1021/acsomega.2c01915
ACS Omega 2022, 7, 18922−18929